JOURNAL OF MATERIALS SCIENCE 24 (1989) 3399–3402

The curvature of amorphous metallic ribbons interpreted with a homogeneous quenching model

F. VARRET, G. LE GAL, M. HENRY
Laboratoire de Spectrométrie Mössbauer UA-CNRS No. 807, Faculté des Sciences, F72017 Le Mans Cedex, France

To explain the curvature of metallic ribbons obtained by quenching techniques, a model is developed in terms of isothermal planar layers, and a well defined solidification plane. Both the cooling rate and the thermal gradient are taken to be constant. Assuming that the ribbon can shrink but not bend during solidification, the resulting curvature is calculated, and is found to equal the thermal gradient multiplied by the linear thermal expansion coefficient. The obtained values compare well with the experimental data. The case of a non-constant thermal gradient is also considered, from a qualitative point of view.

1. Introduction

Metallic amorphous ribbons, obtained either by melt-spinning (narrow ribbons) or by planar-flow casting (wide ribbons), exhibit a sizeable curvature [1–4] with concavity towards their "shiny" side, i.e. their open face (Fig. 1).

The basic reason for this curvature is that successive layers of the ribbon solidify at different times: on the two-layer scheme of Fig. 2, the system returns to room temperature with a lower layer initially colder than the upper layer. This differential effect thus results in a curvature of the two-layer system which is proportional both to the linear thermal expansion coefficient of the material, α_g, and to the initial difference of temperature.

2. Experimental data

Generally, the major curvature is observed in the cross-section plane (Fig. 1); the measurement of this major curvature in the case of narrow ribbons requires the use of a sophisticated roughness meter [5], whereas the measurement of the other curvatures can be made by simple optical means. Our previous studies [3, 4] on a narrow ribbon dealt with the minor curvature. Available experimental data are summarized in Table I.

The occurrence of the major curvature in the ZOY plane can be explained by an earlier solidification of the edges (see also [5]), due to a higher cooling rate [6], which induces additional compressive stresses (see Fig. 3).

There is also good experimental evidence that the quenching process is far from homogeneous [7].

(i) The observed Curie temperature distribution, in the as-quenched state, has been explained by a distribution in the glass temperature T_g whose width should be near 100 K in a narrow ribbon [8]; in such a case, thickness irregularities, correlated with magnetic texture have revealed that transient thermal gradients in the "puddle" could be a major source of inhomogeneity in the solidification process [5]; the liquid "puddle" is schematized on Fig. 4.

(ii) The reversal of curvature after annealing [3, 4] showed that structural relaxation occurred inhomogeneously; this was explained by a glass temperature T_g (and a cooling rate $\dot{T} = dT/dt$) which decreases across the ribbon thickness, from the substrate to the open face.

The thermal gradients corresponding to (i) and (ii) are referred to as "local" and "average", respectively.

A model for inhomogeneous quenching requires a knowledge of the dependence of the glass temperature T_g on the cooling rate $\dot{T}$. So far this crucial function $T_g(\dot{T})$ is not quantitatively known; so, we develop here a simple homogeneous model considering T to be constant (i.e. taking an average $\dot{T}$).

Additional assumptions are needed for the behaviour of the solid layers on which the next layer freezes, *free from stresses*. Here we assume that the ribbon remains flat while freezing; this rigorously occurs if the thermal gradient remains constant during the whole solidification process; stresses responsible for curvature appear later, as the solid ribbon returns to room

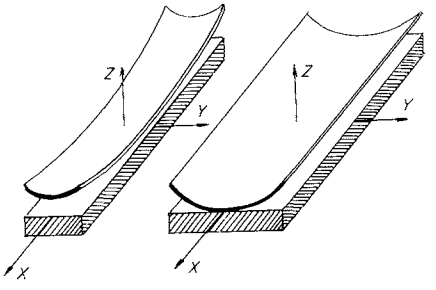

Figure 1 Typical shapes of as-quenched ribbons, prepared with (left) melt-spinning and (right) planar flow technique (the vertical scale is enlarged). The open face ("shiny side") is upwards, and the substrate velocity along the X axis.

0022–2461/89 $03.00 + .12

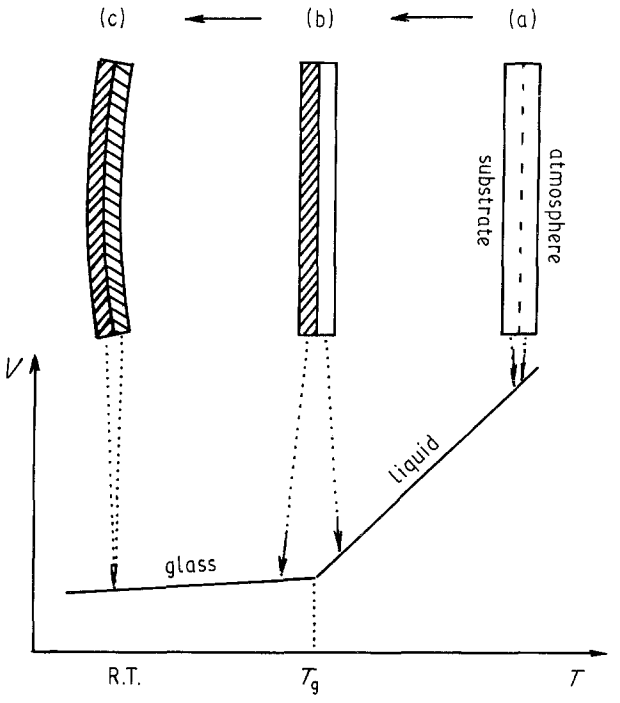

Figure 2 Classical glass formation scheme (volume plotted against temperature), adapted to a two-layer system; the liquid and the glassy states are represented by open and hatched areas, respectively. Stresses occur in the (b) → (c) path, when both layers are solid and undergo different temperature variations.

temperature, with temperature variations differing from layer to layer.

Additional factors acting to maintain the ribbon flat during solidification are the lack of room in the planar-flow casting (Fig. 5) and the weight of the puddle in the melt-spinning technique. We also assume that the ribbon does not stick on the substrate, so that there are no tensile stresses due to the substrate.

This picture is finally equivalent to a two-step process for releasing the thermal stresses of the system: the resulting force is permanently released during solidification; the resulting torque is released after total solidification (then the ribbon bends).

3. A model for homogeneous solidification

The "local" variation of the thermal gradient is neglected, and we consider a solidification plane moving at a constant velocity $\dot{z}_g$ along the z coordinate perpendicular to the substrate. This velocity $\dot{z}_g$ is assumed to be small with respect to the substrate velocity (this will be verified in Section 4), so that the problem can be approximately treated in terms of isothermal planar layers parallel to the substrate.

In addition, we assume in the present section that the "average" variation of the thermal gradient is also

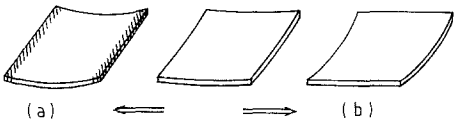

Figure 3 Possible configurations of a bent ribbon after homogeneous quenching: (a) (b) stable equienergetic cylindrical shapes, (c) unstable spherical shape; earlier solidification of the edges (hatched areas) generates compressive stresses whose release favours the shape ***a***.

negligible; for simplicity, we assume that this also applies to the cooling rate so that $\nabla T = \partial T/\partial z$ and $\dot{T} = \partial T/\partial t$ are both taken to be constant. The temperature at position z and time t can then be written

$$T(z, t) = T_0 + \nabla T z + \dot{T} t \quad (1)$$

with $\nabla T > 0$ and $\dot{T} < 0$.

Solidification occurs at position $z_g(t)$ such that $T(z, t) = T_g$ which alternatively leads to

$$z_g(t) = (T_g - T_0 - \dot{T}t)/\nabla T \quad (2)$$

$$t_g(z) = (T_g - T_0 - \nabla T z)/\dot{T} \quad (3)$$

The solidification plane moves at velocity

$$\dot{z}_g = \mathrm{d}z_g(t)/\mathrm{d}t = -(\dot{T}/\nabla T) > 0 \quad (4)$$

Once solidified, any layer starts shrinking according to the linear thermal coefficient α_g, and has length

$$l(z, t) = l(z, t_g(z))[1 + \alpha_g(T - T_g)] \quad (5)$$

The temperature difference written here is only due to the time variation, so that

$$T - T_g = \dot{T}(t - t_g(z))$$

and consequently

$$l(z, t) = l(z, t_g(z))(1 + \alpha_g \dot{T}(t - t_g(z))) \quad (5a)$$

For convenience, this can be rewritten, using Equation 4, as a function of the distance to the solidification plane

$$l(z, t) = l(z, t_g(z))[1 - \alpha_g \nabla T(z - z_g(t))] \quad (5b)$$

The unknown function $l(z, t_g(z)) = l_g(z)$, represents the length of layer z when it freezes, free from stresses. The determination of this function is the aim of the remaining calculations. For this we assume, as previously stated, that the resulting force of the thermal stresses is permanently released so that the solid layers have an average length which is also the length of the next solid layer which solidifies, free from stresses

$$l_g(z) = \frac{1}{z}\int_0^z l(z', t_g(z))\,\mathrm{d}z'$$

$$= \frac{1}{z}\int_0^z l_g(z')[1 + \alpha_g \nabla Y(z' - z)]\,\mathrm{d}z' \quad (6)$$

TABLE I Curvature data on as-quenched metallic ribbons, measured in *ZOX*, *ZOY* planes

Composition	Origin	Width (mm)	Thickness (μm)	R_x^{-1} (m^{-1})	R_y^{-1} (m^{-1})
$Fe_{72.5}Cr_{6.5}P_{13.2}C_{7.8}$	Compagnie St Gobain	2	40	0.06(1)[a]	40[b]
$Fe_{40}Ni_{38}Mo_4B_{18}$ "2826MB"	Allied Corp.	25	30	~0	13(1)[c]

[a][4].
[b][9].
[c]Measured by mechanical means.

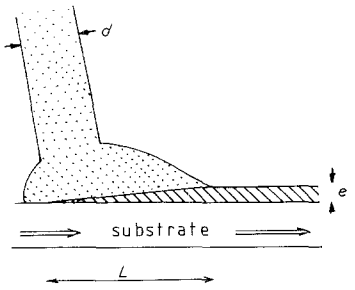

Figure 4 Idealized view of the "puddle" in the melt-spinning devices (with enlarged thickness of the ribbon), adapted from [1]. Typical values for d, L, e are 0.8, 2.5, 0.040 mm, respectively.

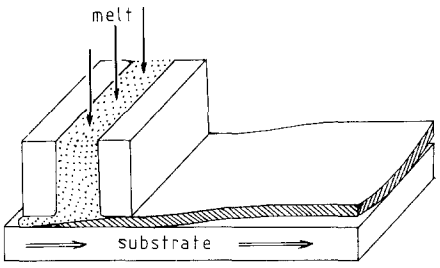

Figure 5 Idealized view of a quenching device (planar flow), with a ribbon which remains flat while freezing, and bends later on.

This integral equation can be solved using a serial development, leading to

$$l_g(z) = l_0[1 - \alpha_g \nabla T z + (\alpha_g \nabla T)^2(z^2/4) + \ldots] \quad (7)$$

where l_0 is an integration constant representing the length of the bottom layer. The return of the ribbon to room temperature introduces a small correction, equal for all layers since they undergo the same temperature change from T_g to T_{room}.

Thus Equation 7 represents the free length of the layers. It explains the cylindrical shape of the ribbon (with OX axis): in the cross-section plane, this shape fits Equation 7 up to the first-order term and allows the stresses to be entirely released. The radius R of the cylinder is such that

$$(l(z) - l(0))/l(0) = z/R$$

A comparison with Equation 7 immediately yields the curvature

$$1/R = \alpha_g \nabla T \quad (8)$$

which appears to be independent of the ribbon width and thickness.

4. Analysis of experimental data

The available data, collected in Table I, allows the determination of the thermal gradient, using Equation 8 and data for the linear thermal expansion coefficient $\alpha_g \approx 1.6 \times 10^{-5}\,K^{-1}$, which is close to that of crystalline iron and nickel, respectively 1.5 and $1.7 \times 10^{-5}\,K^{-1}$

$$\nabla T \sim 2.7 \times 10^6\,km^{-1} \quad \text{for the narrow ribbon}$$

$$\nabla T \sim 8.1 \times 10^5\,km^{-1} \quad \text{for the wide ribbon}$$

Across a thickness e, this leads to a temperature difference between the two sides which is

$$\delta T = e\nabla T \sim 100\,K \quad \text{for the narrow ribbon}$$

$$\sim 24\,K \quad \text{for the wide ribbon.}$$

For further analysis more data is required, in particular the "crossing time" t_c, needed for the solidification plane to cross through the whole thickness.

From a simple observation of the melt spinning device while operating [1], one can observe a "puddle length" L (Fig. 4) of ~ 2.5 mm. Together with the substrate velocity $V \sim 30\,msec^{-1}$ and the thickness $e \sim 40\,\mu m$, this leads to

$$t_c \sim L/V = 8.3 \times 10^{-5}\,sec$$

$$\dot{z}_g = e/t_c \sim 0.48\,msec^{-1}$$

In the absence of similar data concerning the wide ribbon, we shall assume that the velocity of the solidification plane has the same value; this is reasonable since this velocity only depends on the heat transfer coefficient from the substrate, irrespective of the substrate velocity and other quenching parameters. Indeed this value is quite small compared with the substrate velocity (as required previously). From Equation 4 the calculations, summarized in Table II, finally yield

$$\dot{T} = \dot{z}_g \nabla T \sim -1.3 \times 10^6\,K sec^{-1}$$

for the narrow ribbon

$$\sim -0.4 \times 10^6\,K sec^{-1} \quad \text{for the wide ribbon.}$$

These values have the correct order of magnitude, the values usually deduced from thermodynamical models being of some $10^6\,K sec^{-1}$.

Structural relaxation, which is fast near T_g, should tend to reduce the thermal stresses. It seems that it does not play an important role here; this supports the assumption made in Section 2, that the thermal stresses occur when the temperature is far below T_g (Fig. 6).

On the other hand, using the present analysis, the inhomogeneous character of the solidification can be qualitatively investigated; this is done in the next section.

5. Inhomogeneous model

The assumption made above that both ∇T and $\dot{T}$ are constant does not obey the well known heat-transfer equation

$$\lambda \Delta T - C\dot{T} = 0,$$

where λ and C are respectively the heat transfer coefficient and the heat capacity of the material. In one

TABLE II Quenching parameters and data for explaining the major curvature of as-quenched amorphous metallic ribbons

Composition	R^{-1} (m^{-1})	α_g (K^{-1})	∇T ($K\,m^{-1}$)	δT (K)	$\dot{z}_g$ ($m\,sec^{-1}$)	$\dot{T}$ ($K\,sec^{-1}$)
$Fe_{72.5}Cr_{6.5}P_{13.2}C_{7.8}$	40	1.5×10^{-5}	2.7×10^6	100	0.48	1.3×10^6
$Fe_{40}Ni_{38}Mo_4B_{18}$ "2826MB"	13	1.6×10^{-5}	8.1×10^5	24	(id)	0.4×10^6

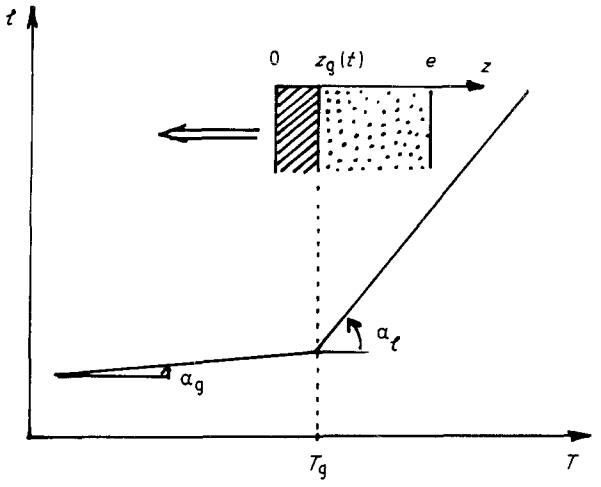

Figure 6 Schematic phase diagram for homogeneous glass formation, showing the thermal dilatations in liquid and glassy states (T_g = glass temperature). The successive layers of the ribbon (hatched = glass) are shown at time t, moving to the left while the ribbon freezes.

dimension, this equation can be written

$$\lambda \frac{\partial^2 T}{\partial z^2} - C\dot{T} = 0 \qquad (9)$$

If $\dot{T}$ is assumed to be negative, this leads to a $\partial T/\partial z = \nabla T$ which is a decreasing function of z. Consequently the crucial function $l_g(z)$ is expected to have a steeper variation near the substrate. As shown in Fig. 7, it is no longer possible to release completely the stresses, and the ribbon remains with both surfaces under compressive stresses (this is similar to the well known quenching effect of glasses).

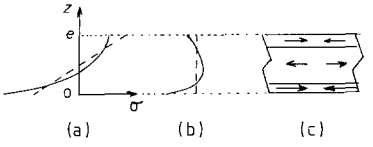

Figure 7 Stress distribution in the case of inhomogeneous quenching (full lines), compared to the case of homogeneous quenching (broken lines): (a) depicts the situation of the ribbon returned to room temperature, but constrained to remain flat, (b) when the torque is released (the ribbon bends); (c) shows compressed and elongated areas, adapted from [3].

6. Conclusion

The present tentative model of homogeneous quenching has explained the correct order of magnitude for the curvature of as-quenched ribbons. A more general model including structural relaxation and inhomogeneous quenching rate is not necessary as long as accurate data concerning the thermodynamics of the solidification are not available.

The values of the temperature difference between the two sides during quenching, $\delta T \sim 100$ K and 24 K, for the narrow and wide ribbon respectively, are of the same order of magnitude as the glass-temperature gradients (100 K, [8]) which can occur transiently in a melt-spinning device. In both ribbons the "local"gradients and the "average" gradients are both present; to separate these two effects, a detailed study of the structural relaxation during thermal annealing should combine "local" observations (such as δT_c measurements) and "average" observations (such as curvature measurements).

Acknowledgement

Acknowledgement is due to Dr J. M. Grenèche for valuable comments and discussions.

References

1. M. HENRY, Thesis, Le Mans, France (1986).
2. M. BOURROUS, Thesis, Le Mans, France (1985).
3. M. BOURROUS and F. VARRET, *J. Magn. Magn. Mater.* **66** (1987) 229.
4. F. VARRET and M. BOURROUS, *Solid State Commun.* **63** (1987) 683.
5. M. BOURROUS, M. HENRY, J. M. GRENECHE and F. VARRET, 5th International Conference on Rapidly Quenched Metals, edited by Steeb and Varlimont (1984).
6. E. VOGT and G. FROMMEYER, *ibid.* p. 63.
7. S. C. HUANG and H. C. FIEDLER, *Met. Trans.* **12A** (1981) 1107.
8. F. VARRET, T. BESNARD and J. M. GRENECHE, *J. Magn. Magn. Mater.* **73** (1988) 157.
9. M. HENRY, M. BOURROUS, F. VARRET and P. FOURNIER, *J. Mater. Sci.* **19** (1984) 1000.

Received 15 March
and accepted 28 July 1988